A comprehensive moment magnitude catalog for the Northeastern Italy region

Gabriele Tarchini (1,2), Luca Moratto (2), Angela Saraò (2)

(1) University of Genoa, Department of Earth, Environmental and Life Sciences, Genoa, Italy

(2) National Institute of Oceanography and Applied Geophysics – OGS, Trieste, Italy

Corresponding author:

Gabriele Tarchini,

Department of Earth, Environmental and Life Sciences (DISTAV), University of Genoa, Viale Benedetto XV 5, 16132 Genoa, Italy

Also at: National Institute of Oceanography and Applied Geophysics – OGS, Borgo Grotta Gigante 42c, 34010 Sgonico, Trieste, Italy

gabriele.tarchini@edu.unige.it

Declaration of Competing Interests

The authors acknowledge that there are no conflicts of interest recorded.

Abstract

We present a comprehensive catalog of independent moment magnitude (M_w) estimates for northeastern Italy and its neighboring regions using data from the OGS (OX) network. The catalog, spanning from 2016 to 2023, covers the geographical area between 10.0°–14.5° north latitude and 44.5°–47.0° east longitude. In this region, we identified 11,685 low-to-moderate magnitude earthquakes ($-0.70 \leq M_L \leq 4.35$) suitable for independent M_w computation. To enhance accuracy, we incorporated new homogeneous estimates of local magnitude (M_L). A newly developed routine enables rapid near real-time M_w estimation and permits regular, rolling seismic catalog updates. We also established an empirical relationship between M_w and M_L specific to our study region.

Our study provides a detailed and accurate M_w catalog of independent estimates that significantly improves critical applications such as seismic hazard assessment, and risk mitigation in this seismically active region. Regular updates will be made as new data becomes available, ensuring ongoing accuracy and relevance. The catalog is accessible online to the scientific community, fostering collaboration and further research, thereby enhancing our understanding of the geodynamics and seismic hazards in northeastern Italy and its surrounding areas.

Keywords: Moment magnitude (M_w); Local magnitude (M_L); Earthquake catalog; Northeastern Italy seismicity; Empirical M_w–M_L relationship; Seismic data analysis.

1. Introduction

Accurately estimating the energy released during seismic events is crucial for understanding the processes that generate both small and large earthquakes. The moment magnitude (M_w), derived from the seismic moment (M_0), serves as a key measure for quantifying this energy. It is considered the most reliable magnitude scale because it does not saturate at large magnitudes (Hanks and Kanamori, 1979) and can be directly related to the properties of the earthquake fault (e.g., Aki, 1967). Estimation of M_w by moment tensor solutions is based on strong ground motions and is effective above a certain magnitude threshold (~3.5–4.0). However, reliably estimating M_w for small seismic events can be challenging, especially for local networks, due to various factors such as signal noise, limited data availability, and poor knowledge of the propagation medium properties. Therefore, M_w estimates for weak events often rely on spectral methods based on corrected source frequency-amplitude spectra (e.g., Andrews, 1986) or response spectra (Atkinson et al., 2014).

Accurately computing M_w plays a significant role in seismic hazard studies by identifying areas with increased seismic activity, improving magnitude-recurrence relationships, refining ground motion prediction equations, and supporting decision-making for subsurface activities that might induce seismicity, such as oil exploration, gas storage, and geothermal resource exploitation. Consequently, numerous researchers have created homogeneous M_w catalogs for various regions (e.g., Grünthal and

Wahlström, 2003; Braunmiller et al., 2005; Karimiparidari et al., 2013; Arabasz et al., 2016; Onur et al., 2017; Das and Meneses, 2021; Peach et al., 2024). M_w is the preferred magnitude for the catalog for two key reasons: (1) almost all contemporary ground-motion prediction equations are expressed in terms of M_w, and (2) M_w provides a more accurate quantification of earthquake size, especially for large earthquakes, where other magnitude scales often saturate. Therefore, it is crucial to include direct M_w calculations whenever possible, rather than relying on conversions from other magnitude scales, particularly for large earthquakes. The vast majority of these catalogs predominantly harmonize M_w values derived from other magnitude scales or macroseismic parameters by using pre-existing or specifically calibrated conversion relationships. Nevertheless, with rapid data transmission to data centers and swift data analysis procedures, it is now possible to reliably and directly estimate earthquake parameters such as M_0 and M_w, with results promptly published online (e.g., Spallarossa et al., 2021; Costa et al., 2022).

In this study, we computed independent M_w for low-to-moderate magnitude earthquakes ($M_w \leq 4.0$) in northeastern Italy and the surrounding areas (Fig. 1), a region that is particularly prone to seismic activity due to its tectonic setting. The interaction between the Adriatic microplate and the Eurasian plate in this area leads to frequent earthquakes, ranging from minor tremors to major seismic events (e.g., Slejko et al., 1989; Sandron et al., 2023). The seismicity, primarily located in the upper crust, is minor and directly related to deformation along the western margin of the Adriatic indentation (e.g., Cheloni et al., 2014; Bressan et al., 2016; Rebez et al., 2024). The strongest recorded earthquake in this area was the May 6, 1976, Friuli earthquake, with a surface-wave magnitude (M_S) of 6.5 (Aoudia et al., 2000). This event caused approximately 1000 deaths and widespread devastation in small villages (Slejko, 2018). Instrumental seismological monitoring in this area began in the late 19th century with the Trieste station, which initially became a reference station and later part of the World-Wide Standardized Seismograph Network (Sandron et al., 2015). Since 1977, the Seismological Research Center of the National Institute of Oceanography and Applied Geophysics (OGS) has been monitoring this region, complementing the national seismic monitoring activities led by the Istituto Nazionale di Geofisica e Vulcanologia – INGV (Bragato et al., 2011; Priolo et al., 2015; Bragato et

al., 2021). The OGS seismic network (international code OX) integrates real-time seismic data from its own stations with those belonging to neighboring seismic networks (Fig. 1).

Since the establishment of the network in 1977, annual seismic bulletins have been consistently published and are available online on the CRS website (Bulletin of the Seismometric Network of North Eastern Italy, 2024). For each earthquake, the location and the duration magnitude (M_D) is given in the bulletin, calculated according to the formulas of Rebez and Renner (1991). With the advent of digital measuring devices, it has become possible to directly estimate the M_L, with precise calibration for the study area (Bragato and Tento, 2005). Since 2009, the seismic moment tensor for earthquakes with a magnitude of $M_L \geq 3.6$ has been calculated in near real-time (Saraò et al., 2021) and the obtained M_w and fault plane solutions have been incorporated into the focal mechanism catalog of the area (Saraò et al., 2021; Sugan et al., 2024).

In line with these advancements, we have recently calculated the M_w of selected seismic events recorded in the study area from January 1, 2016, to December 31, 2023 using the stations of the OX network and other surrounding networks and the method proposed by Atkinson et al. (2014). This approach, which relies on the calculation of response spectra, has already been calibrated for Northeastern Italy (Moratto et al., 2017) and applied in other seismic regions affected by underground gas storage (Lanzoni et al., 2020) and volcanic activity (Saraò et al., 2023). Our new direct estimates of M_w are documented in a freely accessible dataset provided with this article (Moratto et al., 2024), which also includes new homogeneous estimates of M_L, utilizing the region-specific calibration by Bragato and Tento (2005).

In the following sections, we describe the methodologies used to compute M_w and M_L, the data utilized, and the results of the analysis of the selected seismic events included in the M_w dataset (Moratto et al., 2024).

2. Methodology

2.1 M_w computation

To compute M_w, we applied the approach based on response spectra put forward by Atkinson et al. (2014) and calibrated for our study region by Moratto et al. (2017). We calculated the M_w using response spectra computed from vertical waveforms recorded within an epicentral distance of 80 km; since this approach adopts the point-source model (Atkinson et al., 2014), we limit our analysis to earthquakes with $M_w \leq 4.0$. Bora et al. (2016) found that the scaling of response spectra and Fourier Amplitude spectra (FAS) are equivalent at frequencies below the peak of the response spectra. While FAS offers clear advantages, particularly its ability to directly represent waveforms across the entire frequency range without being affected by 1D oscillator filtering, spectral acceleration (SA) remains highly valuable due to its strong correlation with structural response, its widespread use in seismic hazard assessments, and its availability in real-time applications such as ShakeMap parameters. Additionally, response spectra inherently smooth out irregularities in the frequency domain because fluctuations are constrained by the 5% damping applied in their calculation (Atkinson et al., 2014; Moratto et al., 2017). Atkinson et al. (2014) have shown that the pseudo-acceleration amplitude (PSA) calculated at 1.0 s and 0.3 s provides stable representations of the low-frequency motion that correlate well with the seismic moment. For events with $M_w < 4$, frequencies around 1.0 s (1.0 Hz) lie within the low-frequency plateau of a standard Brune (1970) point-source displacement spectrum, where the amplitude is directly proportional to the seismic moment. The Brune model is commonly applied to small-magnitude earthquakes, though its validity largely depends on the quality of the recorded data. For very small events, high-frequency signals can be obscured by noise, making it challenging to reliably estimate source parameters such as corner frequency and seismic moment. Additionally, deviations from self-similarity may arise due to factors such as heterogeneous stress drops, rupture nucleation effects, or local site-specific conditions. Despite these limitations, several studies demonstrated that the Brune model can be effectively applied to magnitudes as low as $M_w \sim 0$, provided that the data quality is sufficiently high (e.g., Abercrombie, 1995). For smaller events ($M_w <$ 3), however, the noise becomes significant and can lead to an overestimation of the magnitude. In

such cases, it is recommended to replace the response spectra calculated at 1.0 s with those calculated at 0.3 s to limit the noise influence on the M_w estimations; in this case, indeed, response spectra computed at 0.3 s perform better, as they are less sensitive to noise.

In this study, we followed the approach developed by Moratto et al. (2017), who used response spectra in the form of absolute spectral acceleration (SA). In general, the SA is approximately equal to the PSA and is considered almost identical for most engineering applications with five percent damping (Mohraz and Sadek, 2001). The attenuation function relating the M_w values to the SA is therefore expressed as follows:

$$\log(SA)_T = a \times M_w - g(R) - b_T \times R + c_T, \quad (1)$$

in which T is the period (0.3, 1.0 s), a is the scaling magnitude parameter, g(R) is the geometrical spreading, b_T refers to the anelastic attenuation, c_T is a constant defined separately for response spectra at 0.3 and 1.0 s (SA03 and SA10, respectively), and R is the hypocentral distance.

Ideally these parameters would be estimated directly from the data. However, due to the lack of reliable M_w estimates for weak events, Atkinson et al. (2014), and Moratto et al. (2017) adopted a two steps procedure. (1) The value of a is determined by computing synthetic seismograms assuming a Brune point source model using a stochastic approach (Boore, 1983, 2003); and (2) the values of b_T and c_T are estimated performing an empirical calibration using a dataset of independent estimates of M_w associated with SA03 and SA10 obtained from the recorded data. Moratto et al. (2017) calculated the synthetic seismograms for wide ranges of magnitude (from 0 to 4, with a step size of 0.2) and hypocentral distance (from one to two hundred kilometers with a step size of 0.1 in the base-10 logarithmic scale) using the Stochastic-Method SIMulation code (Boore, 2003). They employed a ground-motion model specifically designed for northeastern Italy, incorporating regional attenuation and amplification effects. The input parameters for the stochastic simulations were derived from the work of Malagnini et al. (2002), who modeled the spectral propagation of seismic waveforms in the study region. They also used a density of 2.8 g/cm^3, a shear-wave velocity of 3.5 km/s and a high-frequency attenuation parameter (κ) of 0.045 s. Additional parameters relevant to the simulations are detailed in Moratto et al. (2017). The resulting spectral accelerations at 1 Hz (SA10) and 3.3 Hz

(SA03) showed similar trends with distance, therefore based on the simulation results, they averaged the scaling values of a across all magnitudes and distances, yielding a fixed value of 1.49 for Equation (1). This approach provides a robust representation that reflects the overall scaling behavior across the full magnitude range, while acknowledging potential variability in a for specific magnitude ranges.

In calculating the M_w we adopted a cutoff distance of 80 km as recommended by Moratto et al. (2017), to minimize potential regional effects and complexities associated with path propagation (e.g., the Moho reflections observed by Bragato et al., 2011).

The relationships calibrated by Moratto et al. (2017) for northeastern Italy are:

$$M_w(SA10) = (\log(SA10) - D(r, 40, 1.0) + 6.63) / 1.49 \quad \text{for } 2.6 \leq M_w \leq 4.0, \tag{2}$$

$$M_w(SA03) = (\log(SA03) - D(r, 40, 3.3) + 5.38) / 1.49 \quad \text{for } M_w < 2.6, \tag{3}$$

in which $D(r, 40, f)$ is the propagation term at the reference distance $r_{ref} = 40$ km for the periods of interest, defined according to Malagnini et al. (2002) as:

$$D(r, r_{ref}, f) = \log(g(r)) - \log(g(r_{ref})) - ((\pi f (r - r_{ref}) \log(e)) / (\beta Q(f))), \tag{4}$$

in which β is the shear-wave velocity and:

$$Q(f) = 260 (f / 1.0)^{0.55} \tag{5}$$

is the frequency attenuation.

To calculate the response spectra, we used the Covariance Invariant Digital Filtering Technique (Ehrenberg and Hernandez, 1981). This method calculates the maximum absolute acceleration response given an input acceleration trace, the pulsation (the angular frequency ω corresponding to the natural vibration period considered) and the damping constant of the sensor. Since the lower limit of M_w is determined when the signal is overlaid by background noise, which leads to overestimations, only the recordings that exceed a predefined signal-to-noise ratio (SNR) threshold are used to estimate the M_w and the M_L values; the SNR threshold is fixed to 3, independently of the magnitude value. For the identification of the windows over which to calculate the SNR ratio, the revised P-wave arrival times retrieved from the CRS-OGS bulletins are used. In addition, prior to the M_w and M_L calculation, outliers are consistently identified and removed based on the median absolute deviation of the data.

For each event we compute M_w(SA10) and M_w(SA03) applying equations (2) and (3); the final M_w value is M_w(SA10), but this reference magnitude switches to M_w(SA03) when M_w(SA10) is lower than 2.6 (Moratto et al., 2017). For each event, we report the M_w value obtained as the arithmetic average of individual station M_w values, along with the associated standard deviations. This approach relies exclusively on vertical components, as vertical-component spectral acceleration is generally comparable to unamplified horizontal-component spectral acceleration (Lermo and Chavez-Garcia, 1993; Siddiqqi and Atkinson, 2002; Atkinson and Boore, 2006). Atkinson et al. (2014) recommended the use of vertical components because they are less influenced by site response, making this method particularly suitable for a wide range of sites, including those with unknown or poorly characterized site conditions.

2.2. M_L computation

To enrich the catalog, we estimated the M_L values and their associated standard deviations using the calibration relation by Bragato and Tento (2005) for northeastern Italy. This relation is applicable for hypocentral distances ranging from 10 to 250 kilometers and defines $M_L = 3$ as corresponding to a peak amplitude of 10 millimeters on a Wood-Anderson instrument at a hypocentral distance of 17 kilometers. We synthesized equivalent Wood-Anderson seismograms for the north–south and east–west traces, considering the geometric mean of the zero-to-peak values of the two horizontal components. For each event, the M_L value was obtained as the mean value of the M_L values calculated at each station.

3. Data

We processed 12,121 seismic events that occurred between January 1, 2016 and December 31, 2023 in northeastern Italy and neighboring regions. From this dataset, we selected only the earthquakes located within the study area, delineated by the black rectangle in Fig. 1, which is routinely monitored by the CRS-OGS. This selection criteria resulted in a final seismic catalog containing 11,805 earthquakes in the magnitude range of $-0.70 \leq M_L \leq 4.54$. The majority of events have magnitudes

between 0.0 and 2.0, with a peak frequency around 0.5 (Fig. 2). The count decreases significantly for magnitudes above 2.0, indicating a lower occurrence of higher magnitude events.

The location parameters and the reference M_L values of these earthquakes—calculated according to the scale calibrated by Hutton and Boore (1987)—were sourced from the CRS-OGS bulletins (Snidarcig et al., 2016, 2017, 2018, 2019, 2020, 2021; Brondi et al., 2022 —https://rts.crs.inogs.it/it/home.html). The 1D layered velocity model used by the HYPO71 location program (Lee and Lahr, 1975), routinely run for the CRS bulletin, is applied to all the events. This model consists of three layers with P-wave velocities (Vp) of 5.85 km/s, 6.80 km/s, and 8 km/s, and discontinuities at depths of 22 km and 39.5 km, with a Vp/Vs ratio of 1.78 (Riggio and Russi, 1984; Bressan et al., 2003).

Velocimetric three-component waveforms (sampling rate 100 Hz) recorded from ninety-nine stations of the OX network (Bragato et al., 2021) and other seismic networks (see Data and Resources for details), forming the integrated seismometric network in north-eastern Italy, were used to calculate the response spectra and the peaks extracted from the simulated Wood-Anderson seismograms.

Each velocity recording was band-pass filtered in the 0.02–44 Hz frequency range prior to instrument response correction. A newly developed automatic Python procedure processed the waveforms, generating instrument response corrected three-component waveforms tailored to the dataset. The first derivative of the vertical component recordings was then calculated to obtain acceleration waveforms, which were used to compute the response spectra. The corrected broadband waveforms were then filtered to simulate Wood-Anderson seismograms using a static magnification of 2080 (Uhrhammer et al., 1996; Bormann, 2002).

4. Results

After the data selection process on 12,121 seismic events described in the previous section, we obtained M_w values for 11,685 earthquakes and M_L values for 11,564 events. Both estimates are available for 11,444 low-to-moderate magnitude earthquakes ($M_w \leq 4.0$); we estimated no magnitude values for 117 earthquakes due to high noise level or source–receiver distance larger than 80 km. Our catalog for seismic events in northeastern Italy includes detailed information on the location of the

events, the M_D, M_L from bulletins, and the newly computed M_w (both M_w(SA) and M_w(TDMT)) and M_L (Moratto et al., 2024).

The histogram in Fig. 3 illustrates the frequency and distribution of seismic events based on M_w computed in the studied region. The distribution is right-skewed, peaking between magnitudes 1.2 and 1.5, with a significant drop in events for magnitudes greater than 2.0 and few events exceeding 3.0.

The comparison between the two sets of M_L values shows a consistent relationship between M_L(B&T) (Bragato and Tento, 2005) and M_L(H&B) (Hutton and Boore, 1987), with most data points clustering around the 1:1 correlation line (Fig. 4). However, semiparametric spline fit shows deviations, especially at magnitudes lower than 1.0 and for events with $M_L > 3.5$, suggesting slight discrepancies between the two estimation methods. These discrepancies may stem from the calibration of the M_L relationship by Bragato and Tento (2005), which is primarily based on earthquakes with $M_L < 3.0$. Moreover, it is worth mentioning that the Hutton and Boore relationship was defined according to attenuation in Southern California.

4.1 Calibrating M_w–M_L

The comparison of the calculated M_w(SA) with the set of M_L values from different relationships (Figs 5a and 5b) illustrates a strong correlation between M_w(SA) and M_L. However, the deviations from the regression line are less pronounced for the M_L values estimated using the Bragato and Tento (2005) relationship, especially for smaller earthquakes (Fig. 5a). This suggests a more consistent relationship between M_w(SA) and M_L(B&T) values. To a certain extent, this behavior is relatively unsurprising, considering that the relationship of Bragato and Tento was calibrated specifically for the study area, unlike the Hutton and Boore's scale.

The relationship between M_w(SA) and M_L(B&T), computed using orthogonal regression on the 11,444 events with $M_w \leq 4.0$ for which both magnitude estimates are available, is as follows:

$$M_w(SA) = 0.7028\ (\pm\ 0.0018) \times M_L + 0.6814\ (\pm\ 0.0022), \quad (6)$$

while the analogous relationship between M_w(SA) and M_L(H&B), calculated in this case for 11,137 events, is:

$$M_w(SA) = 0.6496\ (\pm\ 0.0024) \times M_L + 0.8240\ (\pm\ 0.0027). \quad (7)$$

The coefficients in equation (6) closely resemble those reported by Moratto et al. (2017). The slope of the relationship ($0.70 \approx 2/3$) matches the scaling parameter proposed by Hanks and Kanamori (1979) and Hanks and Boore (1984). For values in the range $2.0 < M_L < 3.0$, M_L and M_w exhibit closer agreement, with a consistent 1:1 magnitude scaling (Fig. 5a). Below 2.0, the scaling shifts to 2:3, likely due to anelastic attenuation affecting signal propagation paths (Deichmann, 2006, 2017; Bethmann et al., 2011; Moratto et al., 2017). Similar tendencies can be observed for the relationship between M_w(SA) and M_L(H&B) (Fig. 5b), although the deviations from the regression line are more pronounced. Although M_L and M_w scales should reflect the same earthquake properties, deviations between M_L and M_w are common, especially for smaller earthquakes. These deviations can result from various factors, including source and rupture characteristics (e.g., radiation patterns, rupture velocities, rupture directivity, stress drop) as well as instrument or path effects (Deichmann, 2006; Deichmann, 2017; Moratto et al., 2019; Saraò et al., 2023).

To validate our findings, we compared moment tensor solutions for nineteen events that occurred between 2016 and 2023 with the M_w values from our study (Fig. 6a). The mean absolute difference between our M_w values and those computed by Saraò et al. (2021) using time-domain moment tensor (TDMT; Dreger, 2003) analysis is 0.066, with a standard deviation of 0.157. Residuals are nearly symmetrical around a mean of –0.041, with a standard deviation of 0.071 (Fig. 6b), indicating that the differences fall within the empirical uncertainty associated with moment tensor calculations. The largest discrepancy (0.18) was observed for a June 4, 2017 event near Verona (45.6510°N–10.6932°E). The close agreement between our M_w estimates and those independently obtained through TDMT suggests the reliability of our approach in computing M_w.

5. Summary

We provide a comprehensive M_w catalog for seismic events in northeastern Italy, covering a temporal range between 2016 and 2023 in the range $0.50 \leq M_w \leq 3.95$.

Along with the corrected seismic time series, we produced a parametric catalog of the seismic events analyzed (Moratto et al., 2024). For each event, the catalog includes:

- a unique identification code retrieved from the corresponding CRS-OGS bulletin (see Data and Resources), along with the location parameters (latitude, longitude and depth) and the M_D and M_L values taken from the bulletins;
- the mean value, with the corresponding standard deviation, and the median of the M_L values calculated using the scale of Bragato and Tento (2005);
- mean M_w values estimated from response spectra, with the associated standard deviations, calculated using the relations proposed by Moratto et al. (2017); and
- the available M_w(TDMT) values from Sugan et al. (2024).

Using this catalog, we calculated the empirical M_w–M_L relationship for the study area. Our results improve several important applications, including seismic hazard assessment, structural vulnerability evaluation, and disaster mitigation strategies, all of which are essential for risk reduction in this seismically active region. The catalog will be updated regularly as new data becomes available to ensure its accuracy and relevance. The catalog is accessible online to the scientific community to encourage collaboration and further research.

6. Data and Resources

The waveforms utilized in this study are recorded by the following seismic networks: IV (doi:10.13127/sd/x0fxnh7qfy), MN (doi:10.13127/sd/fbbbtdtd6q), NI (doi:10.7914/SN/NI), OE (doi:10.7914/SN/OE), OX (doi:10.7914/SN/OX), RF (doi:10.7914/SN/RF), SI (https://www.fdsn.org/networks/detail/SI), SL (doi:10.7914/SN/SL) and ST (doi:10.7914/SN/ST).

The earthquake locations for the northeastern Italy area are available at https://rts.crs.inogs.it/it/home.html. The continuous waveforms recorded from the OX network are available at http://oasis.crs.ogs.it (Priolo et al., 2015). The processed waveforms and the final M_w catalog can be found at https://doi.org/10.5281/zenodo.12794786 (Moratto et al., 2024). All these websites were last accessed in December 2024.

The map in Fig. 1 has been generated with the Generic Mapping Tools software package (GMT; Wessel et al., 2019); R (R Core Team, 2018) was used to create all other figures.

7. Acknowledgments

Two anonymous reviewers are acknowledged for their constructive comments, which helped improve this article. The authors would like to express their gratitude to Pier Luigi Bragato for his invaluable suggestions and insightful discussions throughout the development of this work. Special thanks are also extended to the technical staff of the Centro di Ricerche Sismologiche (CRS) at the Istituto Nazionale di Oceanografia e di Geofisica Sperimentale (OGS) for their proficient management of the information technology infrastructure and maintenance of the stations.

This study has been supported and partly developed within the Project MEET (Monitoring Earth's Evolution and Tectonics) funded under the National Recovery and Resilience Plan (NRRP); PRIN 2022 project "2022ZHXWC9" – PREPARED (Intercepting the PREparatory Phase of lARge earthquakes from seismic information and gEodetic Displacement); PRIN Project "NASA4SHA" (Fault segmentation and seismotectonics of active thrust systems: the Northern Apennines and Southern Alps laboratories for new Seismic Hazard Assessments in northern Italy).

8. References

Abercrombie, R. E. (1995). Earthquake source scaling relationships from −1 to 5 ML using seismograms recorded at 2.5 km depth, J. Geophys. Res. **100,** 24015–24036, https://doi.org/10.1029/95jb02397.

Aki, K. (1967). Scaling law of seismic spectrum, J. Geophys. Res. **72**, 1217–1231. https://doi.org/10.1029/JZ072i004p01217.

Andrews D. J. 1986. Objective determination of source parameters and similarity of earthquakes of different size, in Earthquake Source Mechanics , Das S. Boatwright J., and Scholz C. H. (Editors), Vol. 6, Geophysical Monograph Series, American Geophysics Union, Washington, D. C. 259–267. https://doi.org/10.1029/GM037p0259.

Aoudia, A., A. Saraò, B. Bukchin, and P. Suhadolc (2000). The 1976 Friuli (NE Italy) thrust faulting earthquake: a reappraisal 23 years later, Geophys. Res. Lett. **27**, 573–576. https://doi.org/10.1029/1999GL011071.

Atkinson, G., and D. Boore (2006). Ground motion prediction equations for earthquakes in eastern North America, Bull. Seismol. Soc. Am. 96, 2181–2205. https://doi.org/10.1785/0120050245.

Atkinson, G., D. Wesley Greig, and E. Yenier (2014). Estimation of moment magnitude (M) for small events (M<4) on local networks, Seismol. Res. Lett. **85**, 1116–1124. https://doi.org/10.1785/0220130180.

Arabasz, W. J., J. C. Pechmann, and R. Burlacu (2016). A uniform moment magnitude earthquake catalog and background seismicity rates for the Wasatch Front and surrounding Utah region—Appendix E, in Working Group on Utah Earthquake Probabilities (WGUEP), 2016, Earthquake probabilities for the Wasatch Front region in Utah, Idaho, and Wyoming: Utah Geological Survey Miscellaneous Publication 16-3, p. E1–E126.

Bethmann, F., N. Deichmann, and P. M. Mai (2011). Scaling relations of local magnitude versus moment magnitude for sequence of similar earthquakes in Switzerland, Bull. Seismol. Soc. Am., **101**, 515–534, https://doi.org/10.1785/0120100179.

Boore, D. (1983). Stochastic simulation of high-frequency ground motion based on seismological models of the radiated spectra, Bull. Seismol. Soc. Am., **73**, 1865–1894. https://doi.org/10.1785/BSSA07306A1865.

Boore, D. (2003). Simulation of Ground Motion Using the Stochastic Method, Pure Appl. Geophys., **160**, 635–676. https://doi.org/10.1007/PL00012553.

Bora, S. S., F. Scherbaum, N. Kuehn, and P. Stafford (2016). On the relationship between Fourier and response spectra: implications for the adjustment of empirical Ground-Motion Prediction Equations (GMPEs), Bull. Seismol. Soc. Am., **106**, 1235–1253, https://doi.org/10.1785/0120150129.

Bormann, P. (ed.) (2002). IASPEI New Manual of Seismological Observatory Practice. ISBN 3-9808780-0-7, GeoForschungsZentrum Potsdam, Vol. 1 and 2, 1250 pp.

Bragato, P. L., and A. Tento (2005). Local Magnitude in Northeastern Italy, Bull. Seismol. Soc. Am. **95,** 579–591, https://doi.org/10.1785/0120040100.

Bragato, P. L., P. Di Bartolomeo, D. Pesaresi, M. P. Plasencia Linares, and A. Saraò (2011). Acquiring, archiving, analyzing and exchanging seismic data in real time at the Seismological Research Center of the OGS in Italy, Ann. Geophys. **54**, 67–75. https://doi.org/10.4401/ag-4958.

Bragato, P. L., P. Comelli, A. Saraò, D. Zuliani, L. Moratto, V. Poggi, G. Rossi, C. Scaini, M. Sugan, C. Barnaba, P. Bernardi, M. Bertoni, G. Bressan, A. Compagno, E. Del Negro, P. Di Bartolomeo, P. Fabris, M. Garbin, M. Grossi, …, and S. Parolai (2021). The OGS- North-Eastern Italy Seismic and Deformation Network: current status and outlook, Seism. Res. Lett. **92**, 1704–1716. https://doi.org/10.1785/0220200372.

Braunmiller, J., N. Deichmann, D. Giardini, S. Wiemer, and Magnitude Working Group (2005). Homogeneous Moment-Magnitude Calibration in Switzerland, Bull. Seismol. Soc. Am. **95**, 58–74. https://doi.org/10.1785/0120030245.

Bressan, G., M. Ponton, G. Rossi, and S. Urban (2016). Spatial organization of seismicity and fracture pattern in NE Italy and W Slovenia, J. Seismol. **20**, 511–534, https://doi.org/10.1007/s10950-015-9541-9.

Bressan, G., P. L. Bragato, and C. Venturini (2003). Stress and strain tensors based on focal mechanisms in the seismotectonic framework of the Friuli–Venezia Giulia region (north-eastern Italy), Bull. Seism. Soc. Am. **93**, 1280–1297, https://doi.org/10.1785/0120020058.

Brondi, P., A. Snidarcig, P. Bernardi, P. L. Bragato, and P. Di Bartolomeo (2022). Bollettino della Rete Sismometrica dell'Italia Nord Orientale (RSINO), [Data set]. Istituto Nazionale di Oceanografia e di Geofisica Sperimentale - OGS, https://doi.org/10.13120/w1vp-b578.

Brune, J. (1970). Tectonic Stress and the Spectra of Seismic Shear Waves from Earthquakes, J. Geophys. Res. **75**, 4997–5009 https://doi.org/10.1029/JB075i026p04997.

Bulletin of the Seismometric Network of North Eastern Italy (last accessed December 2024) (2024). http://www.crs.ogs.it/bollettino_new/

Cheloni, D., N. D'Agostino, and G. Selvaggi (2014). Interseismic coupling, seismic potential and earthquake recurrence on the southern front of the Eastern Alps (NE Italy), J. Geophys. Res. Solid Earth **119**, 4448–4468, https://doi:10.1002/2014JB010954.

Costa, G., P. Brondi, L. Cataldi, S. Cirilli, A. Cuius, D. Ertuncay, P. Falconer, L. Filippi, S. F. Fornasari, V. Pazzi, and P. Turpaud (2022). Near-Real-Time Strong Motion Acquisition at National Scale and Automatic Analysis, Sensors **22**, 5699. https://doi.org/10.3390/s22155699.

Das, R., and C. Meneses (2021). A unified moment magnitude earthquake catalog for Northeast India. Geomatics, Natural Hazards and Risk **12,** 167–180. https://doi.org/10.1080/19475705.2020.1863269.

Deichmann, N. (2006). Local magnitude, a moment revisited, Bull. Seism. Soc. Am. **96**, 1267–1277. https://doi.org/10.1785/0120050115.

Deichmann, N. (2017). Theoretical basis for the observed break in M_L / M_w scaling between small and large earthquakes, Bull. Seismol. Soc. Am. **107**, 505–520. https://doi.org/10.1785/0120160318.

Dreger, D. S. (2003). TDMT_INV: time-domain seismic moment tensor inversion, In: W.H.K. Lee, H. Kanamori, P.C. Jennings and C. Kisslinger (eds.), International Handbook of Earthquake and Engineering Seismology **81** B, 1627 Academic Press, Amsterdam. https://doi.org/10.1016/S0074-6142(03)80290-5.

Ehrenberg, J. E., and E. N. Hernandez (1981). Covariance-invariant digital filtering—A better digital processing technique for ground motion studies, Bull. Seismol. Soc. Am. **71**, 1361–1367. https://doi.org/10.1785/BSSA0710041361

Grünthal, G., and R. Wahlström (2003). An Mw based earthquake Catalogue for central, northern and northwestern Europe using a hierarchy of magnitude conversions, J. Seismol. **7**, 507–531 https://doi.org/10.1023/B:JOSE.0000005715.87363.13.

Hanks, T. C., and H. Kanamori (1979). A moment magnitude scale, J. Geophys. Res. **84**, 2348–2350. https://doi.org/10.1029/JB084iB05p02348.

Hanks, T. C., and D. M. Boore (1984). Moment-magnitude relations in theory and practice, J. Geophys. Res. **89**, 2033–2046. https://doi.org/10.1029/JB089iB07p06229.

Hutton, L. K., and D. M. Boore (1987). The M_L scale in southern California, Bull. Seism. Soc. Am. **77**, 2074 –2094. https://doi.org/10.1785/BSSA0770062074.

Karimiparidari, S., M. Zaré, H. Memarian, and A. Kijko (2013). Iranian earthquakes, a uniform catalog with moment magnitudes, J. Seismol. **17**, 897–911. https://doi.org/10.1007/s10950-013-9360-9.

Lanzoni, A., L. Moratto, E. Priolo, and M. A. Romano (2020). Fast M_w estimation of microearthquakes recorded around the underground gas storage in the Montello-Collalto area (Southeastern Alps, Italy), J. Seismol. **24**, 1029–1043. https://doi.org/10.1007/s10950-019-09889-0.

Lee W. H. K., and Lahr J. C. (1975). HYPO71 (revised): A computer program for determining local earthquake hypocenter, magnitude, and first motion pattern of local earthquakes, US Geological Survey Open-File Report, 75-311, Melon Park, California (113 pp.).

Lermo, J., and F. J. Chavez-Garcia (1993). Site effect evaluation using spectral ratios with only one station, Bull. Seismol. Soc. Am. **83**, 1574–1594. https://doi.org/10.1785/BSSA0830051574.

Malagnini, L., A. Akinci, R.B. Herrmann, N.A. Pino, and L. Scognamiglio (2002). Characteristics of the ground motion in Northeastern Italy, Bull. Seismol. Soc. Am. **92**, 2186–2204. https://doi.org/10.1785/0120010219.

Mohraz, B., and F. Sadek (2001). Earthquake Ground Motion and Response Spectra, in The Seismic Design Handbook, edited by F. Naeim, Van Nostrand Reinhold, Springer, Boston, 47–124.

Moratto, L., A. Saraò, and E. Priolo (2017). Moment Magnitude (M_w) Estimation of Weak Seismicity in Northeastern Italy, Seism. Res. Lett. **88**, 1455–1464. https://doi.org/10.1785/0220170063.

Moratto, L., M. A. Romano, G. Laurenzano, S. Colombelli, E. Priolo, A. Zollo, A. Saraò, and M. Picozzi (2019). Source parameter analysis of microearthquakes recorded around the underground gas storage in the Montello-Collalto Area (Southeastern Alps, Italy), Tectonophysics **762**, 159–168. https://doi.org/10.1016/j.tecto.2019.04.030.

Moratto, L., G. Tarchini, and A. Saraò (2024). Catalog of NE Italy earthquakes M_w with related velocimetric time series [Data set]. Zenodo. https://doi.org/10.5281/zenodo.12794785.

Onur, T., R. Gök, W. Abdulnaby, H. Mahdi, N. M. S. Numan, H. Al-Shukri, A. M. Shakir, H. K. Chlaib, T. H. Ameen, and N.A. Abd (2017). A Comprehensive Earthquake Catalog for Iraq in Terms of Moment Magnitude. Seism. Res. Lett. **88**, 798–811. https://doi.org/10.1785/0220160078.

Peach, C., S. E. J. Nippress, D. Green, K. Mayeda, J. M. Wookey, and M. J. Werner (2024). A UK M_w catalogue derived from coda envelopes, Geophys. J. Int. **238**, 974–991. ggae180. https://doi.org/10.1093/gji/ggae180.

Priolo, E., G. Laurenzano, C. Barnaba, P. Bernardi, L. Moratto, and A. Spinelli (2015). OASIS - The OGS archive system of instrumental seismology, Seismol. Res. Lett. **86**, 978–984. https://doi.org/10.1785/0220140175.

R Core Team (2018). R: A language and environment for statistical computing, R Foundation for statistical computing, Vienna, Austria, available at https://www.r-project.org/ (last accessed July 2024).

Rebez, A., and G. Renner (1991). Duration magnitude for the northeastern Italy seismometric network, Boll. Geof. Teor. App., **33**, 177–186.

Rebez, A., G. Renner, D. Sandron, and D. Slejko (2024). The eastern Alps earthquake catalogue (1977-2022), Bull. Geophys. Ocean. **65**, 115–122. https://doi.org/10.4430/bgo00453.

Riggio, A., and M. Russi, (1984). Procedura di analisi ed elaborazione dei dati registrati da reti sismometriche locali, in: Finalità ed Esperienze della Rete Sismometrica del Friuli-Venezia Giulia, Reg. Aut. Friuli-Venezia Giulia, Trieste, Italy, 53–74.

Sandron, D., G. F. Gentile, S. Gentili, A. Saraò, A. Rebez, M. Santulin, and D. Slejko (2015). The Wood Anderson of Trieste (NE Italy): one of the last operating torsion seismometers, Seism. Res. Lett. **86**, 1645–1654. https://doi.org/10.1785/0220150047.

Sandron, D., A. Rebez, A. Tamaro, and D. Slejko (2023). Recent earthquakes (2000-2021) in and around the FriuliVenezia Giulia region (NE Italy) and quality improvements of the OGS network monitoring capabilities, Bull. Geoph. Ocean. **64**, 237–258. https://doi.org/10.4430/bgo00421.

Saraò, A., M. Sugan, G. Bressan, G. Renner, and A. Restivo (2021). A focal mechanism catalogue of earthquakes that occurred in the southeastern Alps and surrounding areas from 1928–2019, Earth Syst. Sci. Data **13**, 2245–2258. https://doi.org/10.5194/essd-13-2245-2021.

Saraò, A., L. Moratto, E. Giampiccolo, and O. Cocina (2023). Moment magnitude for earthquakes in the area of the Etna volcano, Geophys. J. Int. **234**, 2519–2533. https://doi.org/10.1093/gji/ggad257.

Siddiqqi, J., and G. Atkinson (2002). Ground motion amplification at rock sites across Canada, as determined from the horizontal-to-vertical component ratio, Bull. Seismol. Soc. Am. 92, 877–884. http://dx.doi.org/10.1785/0120010155.

Slejko, D., G. B. Carulli, R. Nicolich, A. Rebez, A. Zanferrari, A. Cavallin, C. Doglioni, F. Carraro, D. Castaldini, V. Illiceto, E. Semenza, and C. Zanolla (1989). Seismotectonics of the Eastern Southern-Alps: a review, Boll. Geof. Teor. App. **31**, 109–136.

Slejko, D. (2018). What science remains of the 1976 Friuli earthquake?, Boll. Geof. Teor. Appl. **59**, 327–350, doi: 10.4430/bgta0224.

Snidarcig, A., P. Bernardi, P. L. Bragato, P. Di Bartolomeo, M. Garbin, and S. Urban (2016). Bollettino della Rete Sismometrica dell'Italia Nord Orientale (RSINO), [Data set]. Istituto Nazionale di Oceanografia e di Geofisica Sperimentale - OGS, Trieste, Italy. https://doi.org/10.6092/a608d853-755e-4177-aada-992857ccb44e.

549

550 Snidarcig, A., P. Bernardi, P. L. Bragato, P. Di Bartolomeo, M. Garbin, and S. Urban (2017).
551 Bollettino della Rete Sismometrica dell'Italia Nord Orientale (RSINO), [Data set]. Istituto Nazionale
552 di Oceanografia e di Geofisica Sperimentale - OGS, Trieste, Italy. https://doi.org/10.6092/3ff3c323-
553 d7a4-4183-bea0-1a53814ac8b9.

554

555 Snidarcig, A., P. Bernardi, P. L. Bragato, P. Di Bartolomeo, M. Garbin, and S. Urban (2018).
556 Bollettino della Rete Sismometrica dell'Italia Nord Orientale (RSINO), [Data set]. Istituto Nazionale
557 di Oceanografia e di Geofisica Sperimentale - OGS, Trieste, Italy. https://doi.org/10.6092/c53f37ce-
558 bcf3-453c-a2cf-1894d48cfbbb.

559

560 Snidarcig, A., P. Bernardi, P. L. Bragato, P. Di Bartolomeo, M. Garbin, and S. Urban (2019).
561 Bollettino della Rete Sismometrica dell'Italia Nord Orientale (RSINO), [Data set]. Istituto Nazionale
562 di Oceanografia e di Geofisica Sperimentale - OGS, Trieste, Italy. https://doi.org/10.6092/58ff169a-
563 2f02-46ae-908a-bdfcacea069c.

564

565 Snidarcig, A., P. Bernardi, P. L. Bragato, P. Di Bartolomeo, M. Garbin, and S. Urban (2020).
566 Bollettino della Rete Sismometrica dell'Italia Nord Orientale (RSINO), [Data set]. Istituto Nazionale
567 di Oceanografia e di Geofisica Sperimentale - OGS, Trieste, Italy. https://doi.org/10.13120/108b8d94-
568 361a-45f3-8195-fc4e8f73d264.

569

570 Snidarcig, A., P. Bernardi, P. L. Bragato, P. Di Bartolomeo, M. Garbin, and S. Urban (2021).
571 Bollettino della Rete Sismometrica dell'Italia Nord Orientale (RSINO), [Data set]. Istituto Nazionale
572 di Oceanografia e di Geofisica Sperimentale - OGS, Trieste, Italy. https://doi.org/10.13120/8b252b09-
573 314f-456f-812a-b05268ecd001.

574

Spallarossa, D., M. Picozzi, D. Scafidi, P. Morasca, C. Turino, and D. Bindi (2021). The RAMONES Service for Rapid Assessment of Seismic Moment and Radiated Energy in Central Italy: Concepts, Capabilities, and Future Perspectives, Seism. Res. Lett. **92** (3): 1759–1772. https://doi.org/10.1785/0220200348.

Sugan, M., A. Saraò, A. Magrin, A. Snidarcig, G. Bressan, G. Renner, M. A. Romano, M. Guidarelli, M. Santulin, P. Di Bartolomeo, and A. Restivo (2024). Focal mechanisms of the Southeastern Alps and surroundings (2.0) [Data set]. Zenodo. https://doi.org/10.5281/zenodo.10853582.

Uhrhammer, R. A., S. J. Loper, and B. Romanowicz (1996). Determination of local magnitude using BDSN broadband records, Bull. Seismol. Soc. Am. **86**, 1314–1330.

Wessel, P., J. F. Luis, L. Uieda, R. Scharroo, F. Wobbe, W. H. F. Smith, and D. Tian (2019). The Generic Mapping Tools Version 6. Geochemistry, Geophysics, Geosystems **20**(11), 5556–5564. https://doi.org/10.1029/2019GC008515

Full mailing address for each author

Gabriele Tarchini

Department of Earth, Environmental and Life Sciences (DISTAV), University of Genoa, Viale Benedetto XV 5, 16132 Genoa, Italy

Also at: National Institute of Oceanography and Applied Geophysics – OGS, Borgo Grotta Gigante 42c, 34010 Sgonico, Trieste, Italy

gabriele.tarchini@edu.unige.it

Luca Moratto

National Institute of Oceanography and Applied Geophysics – OGS, Borgo Grotta Gigante 42c, 34010 Sgonico, Trieste, Italy

lmoratto@ogs.it

Angela Saraò

National Institute of Oceanography and Applied Geophysics – OGS, Borgo Grotta Gigante 42c, 34010 Sgonico, Trieste, Italy

asarao@ogs.it

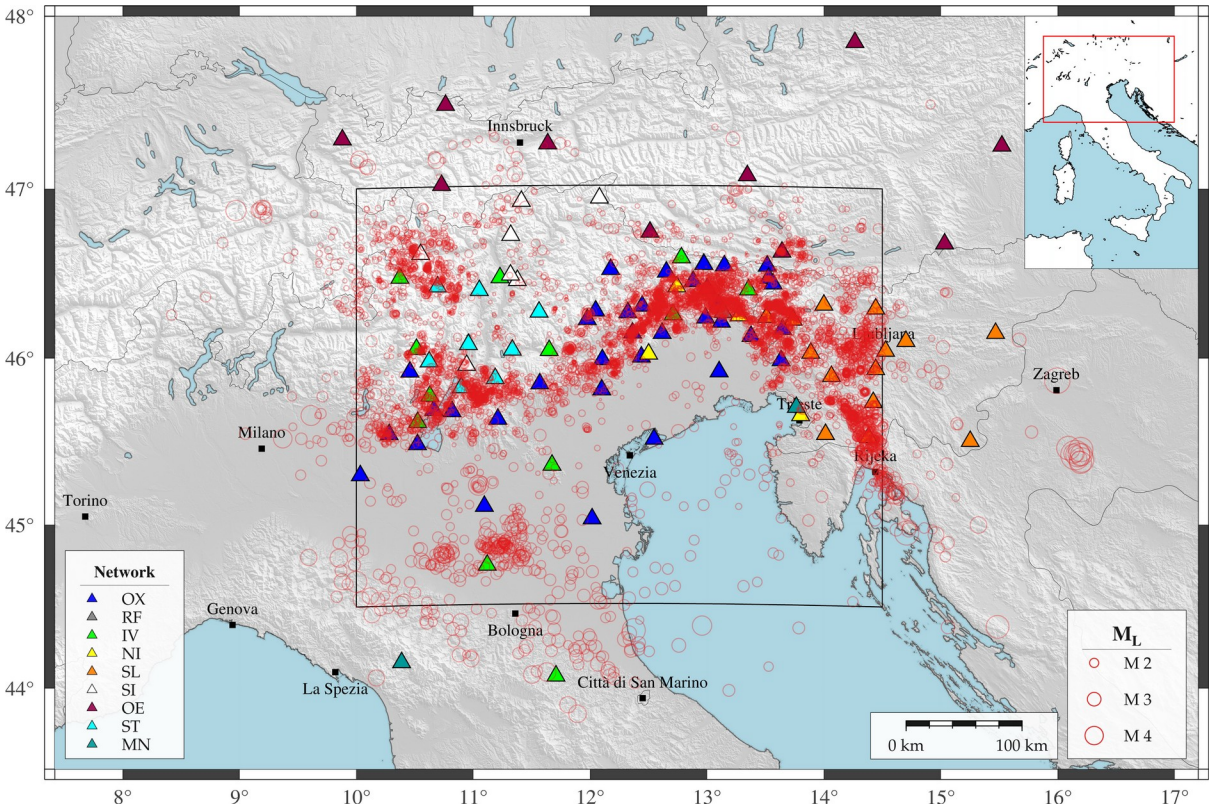

626 **Figure 1.** Map of the seismicity analyzed in this study, represented by circles, with dimensions
627 proportional to the local magnitude values taken from the Centro di Ricerche Sismologiche-Istituto
628 Nazionale di Oceanografia e di Geofisica Sperimentale (CRS-OGS) bulletins. The stations used are
629 from the OX network and other surrounding networks (color-coded according to the legend). The
630 black rectangle marks the study area monitored by the OGS. The inset map shows the location of the
631 study area in Italy, with the red rectangle corresponding to the same geographical extent as the main
632 figure.

633

634

635

636

637

638

639

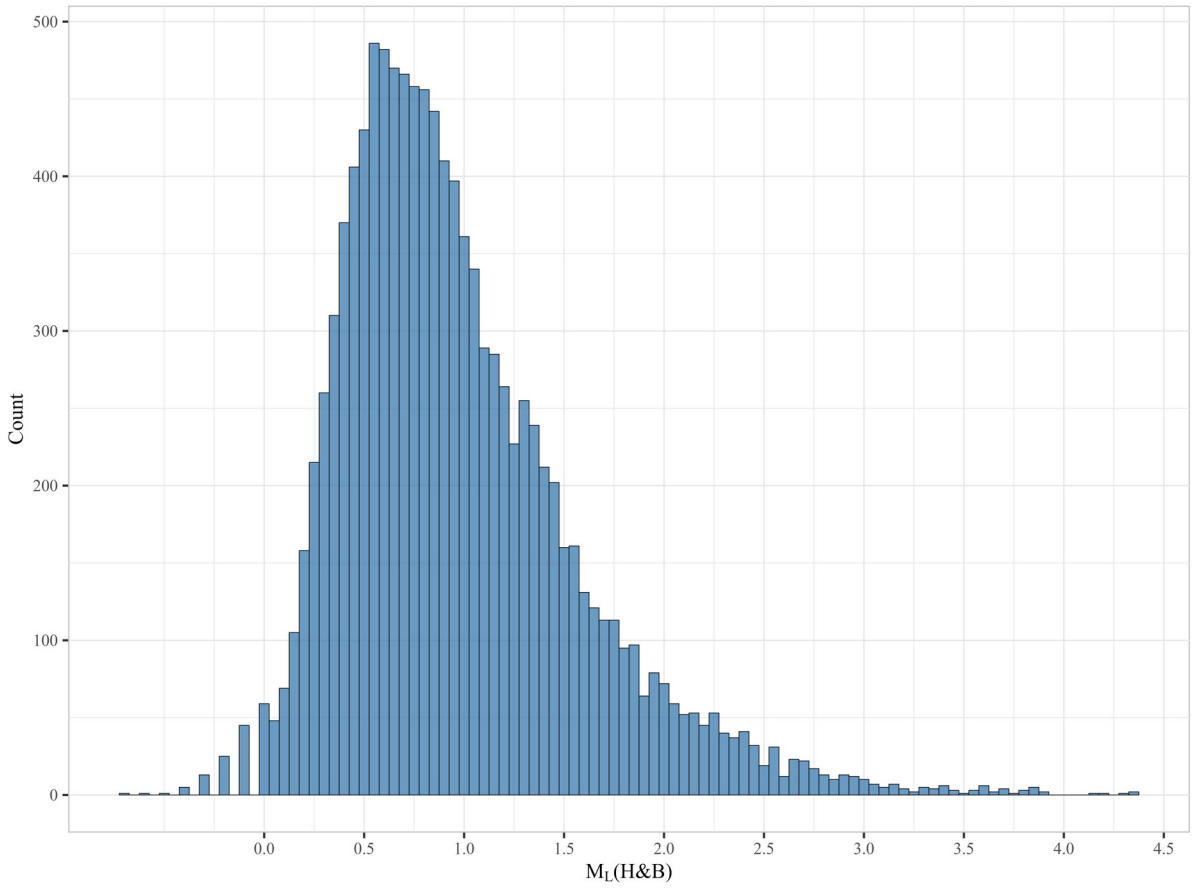

Figure 2. Frequency and distribution of seismic events analyzed in this study based on M_L reported in the CRS-OGS bulletins.

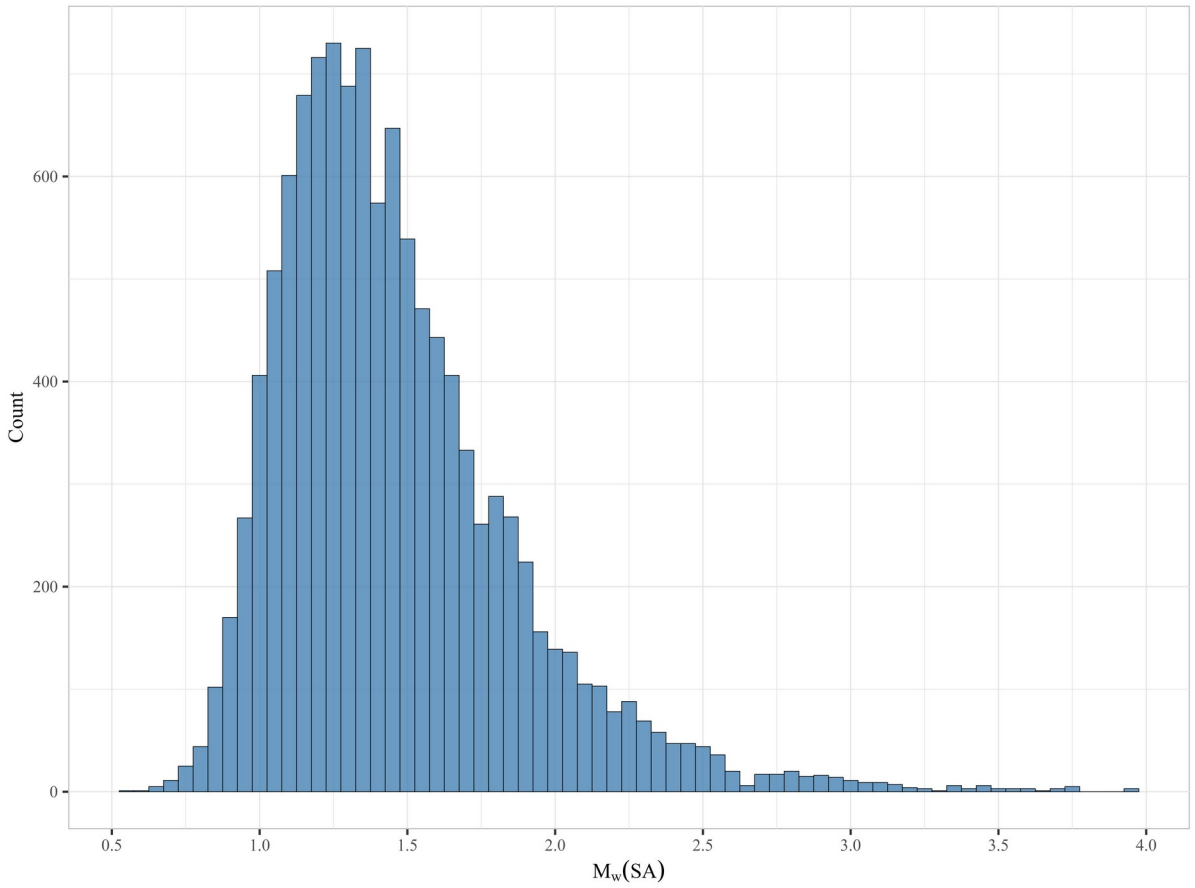

650 **Figure 3.** Histogram illustrating the frequency and distribution of seismic events based on M_w(SA) in
651 northeastern Italy.

652

653

654

655

656

657

658

659

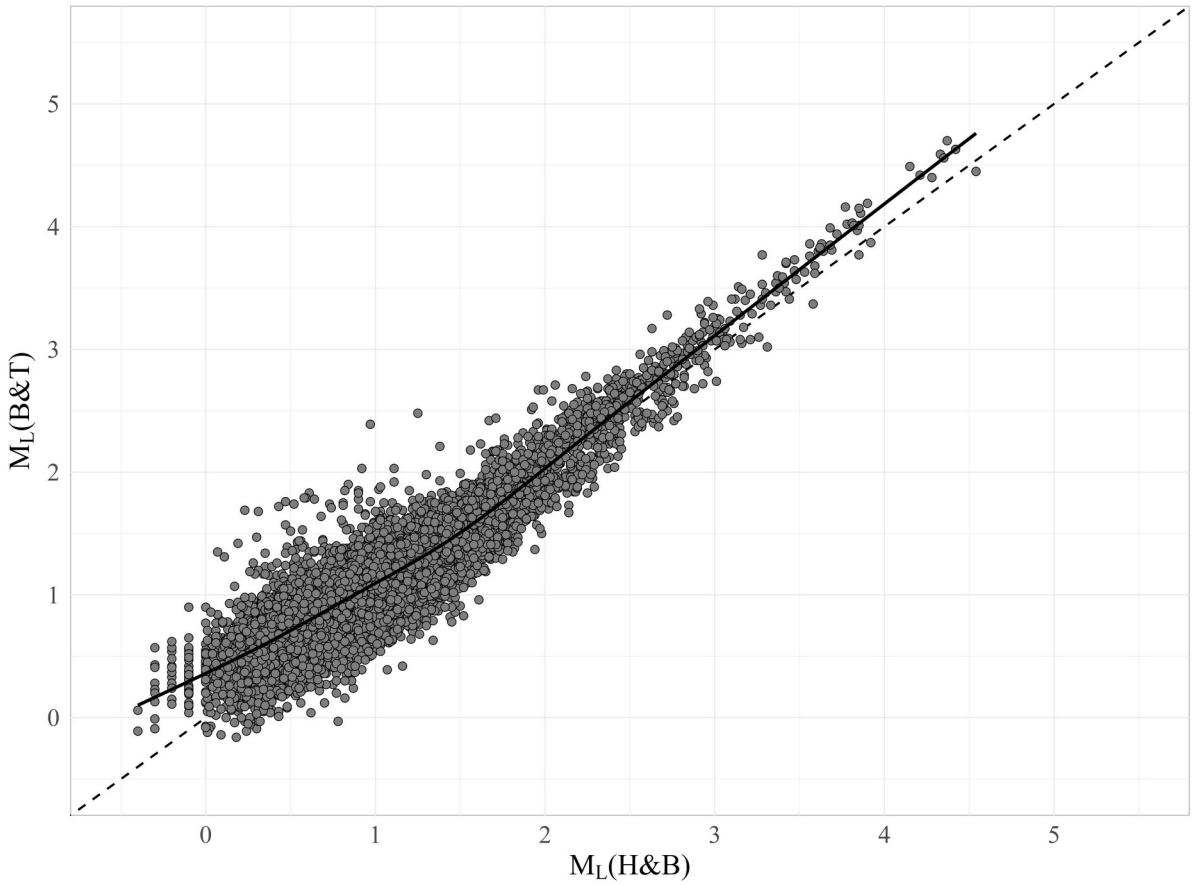

Figure 4. Scatter plot comparing ML values extracted from the CRS-OGS bulletins (ML(H&B)) with ML values estimated using the Bragato and Tento (2005) relationship (ML(B&T)). The dashed line represents the 1:1 correlation, while the black solid line shows the semiparametric spline fit.

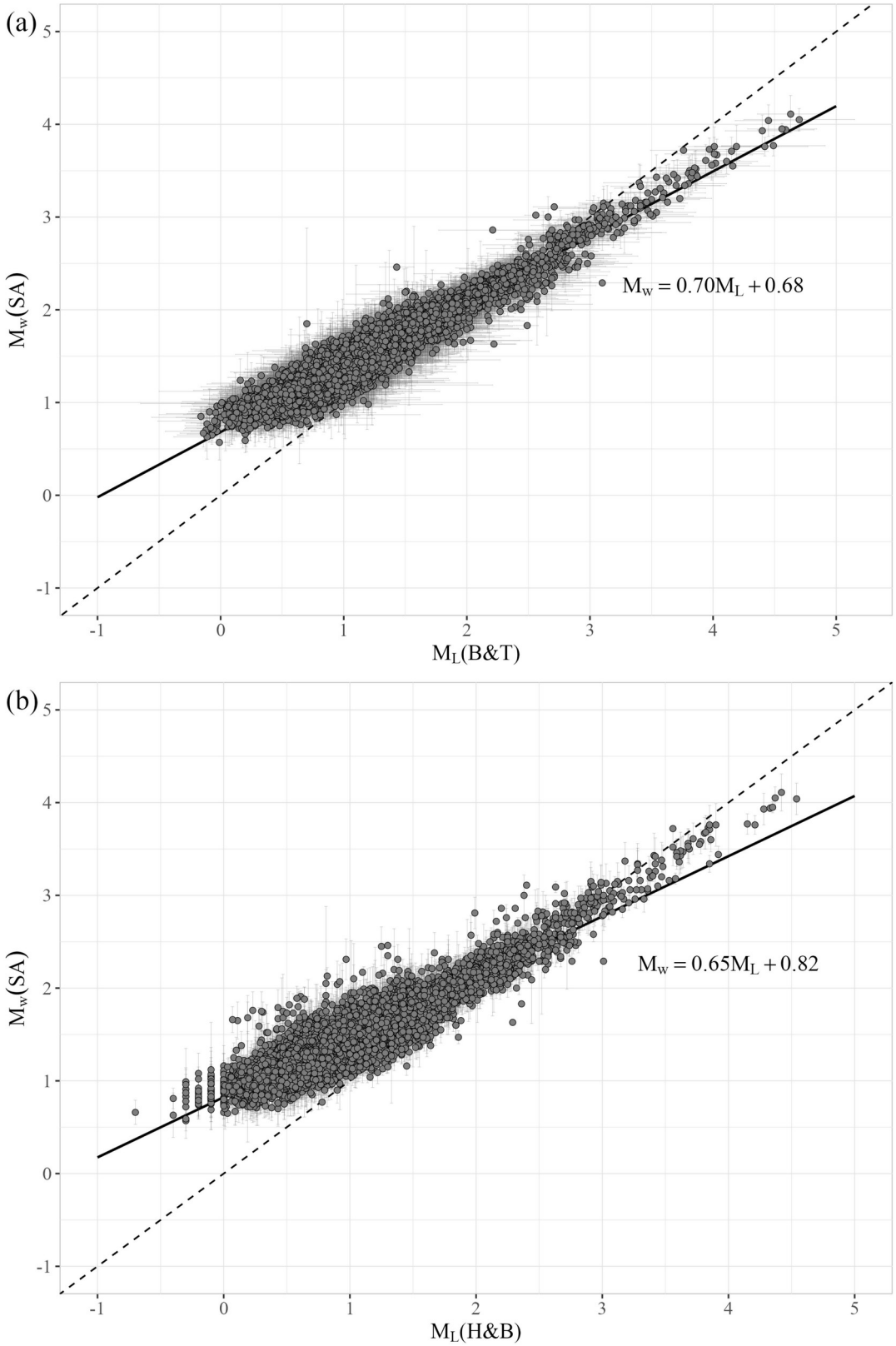

668 **Figure 5. (a)** Scatter plot comparing M_L(B&T) vs M_w(SA). The dashed line represents the 1:1
669 correlation, while the gray solid line indicates the best-fit linear regression, highlighting the overall
670 trend between the two measurements. Error bars for each data point illustrate the variability and
671 uncertainty in the measurements. (**b)** Similar to (**a)**, but comparing M_L(H&B) vs M_w(SA).

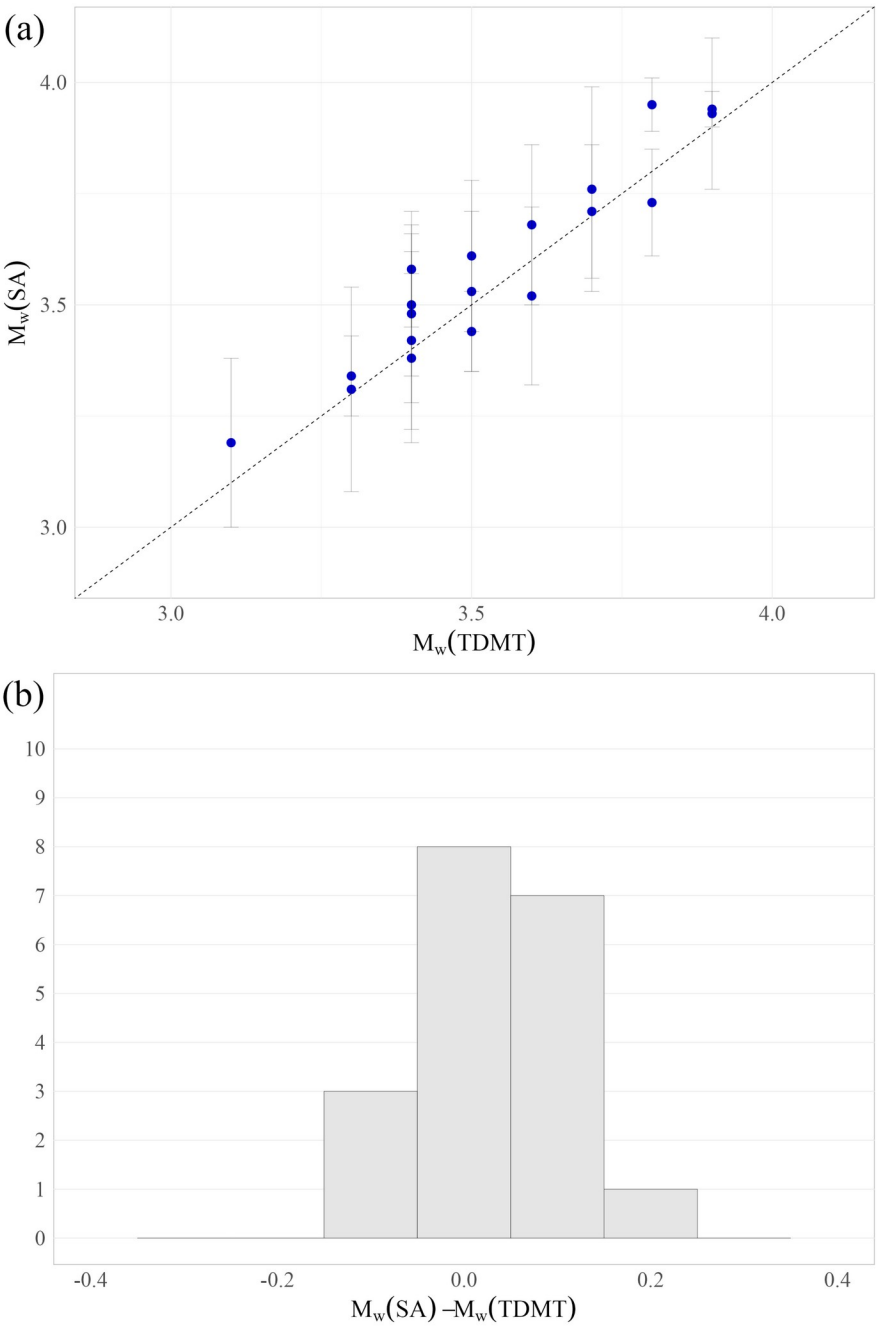

672 **Figure 6.** (**a**) Scatter plot comparing M_w values derived in this study with those computed by Saraò et
673 al. (2021) using time-domain moment tensor (TDMT) analysis in the magnitude range $3.0 \leq M_w \leq$
674 4.0. The dotted line represents the 1:1 correlation. (**b**) Histogram of residuals between our M_w values
675 and those computed by Saraò et al. (2021). The residuals are nearly symmetrical around a mean of –
676 0.041, with a standard deviation of 0.071.